CURRENT SHEET MAGNETIC MODEL FOR THE SOLAR CORONA   *Kenneth H. Schatten*

ABSTRACT   A new magnetic model is developed and compared with previous models and the observed solar corona. An attempt is made to more accurately compute the three-dimensional currents flowing in the solar corona. Physical reasons are given that require most of the large-scale currents flowing in the solar corona to lie near thin sheets. The current sheets are not constrained into any particular geometry or symmetry as in the previous models of *Altschuler and Newkirk* [1969] and *Schatten et al.* [1969]. A comparison with the axisymmetric, isothermal MHD solution of *Pneuman and Kopp* [1970] suggests that the model is able to simulate to high accuracy an isothermal corona. A comparison of the model with the May 30, 1965, solar eclipse and the November 12, 1966, solar eclipse shows the model is capable of computing many features including the polar plume orientations as well as radial and nonradial streamers in the solar corona.

INTRODUCTION

The advent of large digital computers and detailed magnetograms has permitted sophisticated analyses of magnetic field configurations in the vicinity of the sun as suggested by *Gold* [1956]. Computations of the coronal magnetic field utilizing potential theory began with the *Schmidt* [1964] program to plot current-free magnetic fields above active regions. *Rust* [1966] has compared the field configuration of the Schmidt program with direct observations of prominent material. *Newkirk et al.* [1968] utilized potential theory over the entire sun to calculate field patterns for a comparison with the projected appearance of the November 12, 1966 solar eclipse. *Schatten* [1968a,b] and *Schatten et al.* [1969] developed a "source surface" technique to calculate the effect of coronal currents upon the field. The currents were chosen to draw the field into a radial direction (fig. 1). This model allowed comparisons of fields calculated with the interplanetary field, a Faraday rotation eclipse [*Schatten*, 1968a,b 1969, 1970; *Stelzried et al.*, 1970; and *Smith and Schatten*, 1970]. The technique has received favorable review by *Cowling* [1969].

Schatten et al. [1969] utilized a "source surface"

located at 0.6 solar radii above the photosphere. This distance was chosen from a parameteric fit of this quantity based on comparisons of the model with the observed interplanetary field. This would be the location in the model where the highest coronal loops would form. *Bugoslavaskaya* [1950] observed the solar corona from 1887 to 1945, and *Newkirk* [1967] found the highest closed arches have a mean height of 0.6 solar radii above the limb.

Further evidence for the highest closed magnetic loops lying near 0.6 solar radii above the limb is provided by the observations of *Takakura* [1966] that U bursts have a maximum height near this value. U bursts are thought to be essentially type III radio bursts caused by the motion of high speed particles through the solar atmosphere, in which an increase in radio frequency emitted follows the usual decrease. The inversion in radio frequency emitted is interpreted as a decrease in altitude of these particles as they move through the corona on the magnetic field lines which govern their motion.

Although the magnetic models of the corona of *Altschuler and Newkirk* [1969] and *Schatten et al.* [1969] appear to be capable of calculating the large-scale structure of the coronal and interplanetary magnetic fields moderately well, there are two areas

The author is at the Laboratory for Extraterrestrial Physics NASA-Goddard Space Flight Center, Greenbelt, Maryland.

where notable deviations may be found that relate to the magnetic models:

$$\nabla \times \vec{B} = \frac{4\pi \vec{j}}{c}$$

$$\nabla \cdot \vec{B} = 0$$

$B_\theta = 0$

$B_\phi = 0$

$\vec{j} \neq 0$

$\nabla \cdot \vec{M} \neq 0$
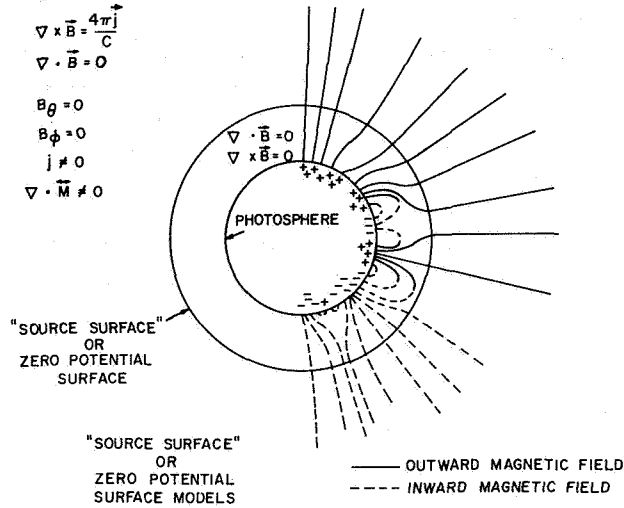
Figure 1. *Magnetic field geometry in the "source surface" or "zero-potential surface" models. The fields are constrained to the radial direction by the solar wind in these models. The equations obeyed in the different regions are shown.*

1. Solar flares appear to affect the large-scale magnetic field of the corona. The influence may appear in a solar eclipse photograph as the formation of series of fine rays directed radially away from the source of the flare [Smith and Schatten, 1970].

2. Although much of the open field structures and closed field structures have the correct topology, the structures are not always directed properly. A notable example is the polar plumes, which appear to bend continually equatorward, whereas the magnetic models orient them in the radial direction at the "source surface" or "zero potential surface". Another example are streamers, whose axes show a preferential lean to the equator near solar minimum and toward the poles at solar maximum [Waldmeier, 1970]. Figure 2 illustrates the nonradial aspects or coronal features.

The first area of disagreement is expected due to the large amount of hot plasma emitted by a flare. The current-free assumption in the inner corona is violated by this hot plasma and thus the potential solution is no longer valid. The second area of disagreement may relate to the latitudinal and azimuthal magnetic pressure terms that are important in coronal structure but have been neglected beyond the zero potential surface in prior work for mathematical simplicity. The purpose of this work will be to improve the model by including this effect. The energy density of the radial magnetic field
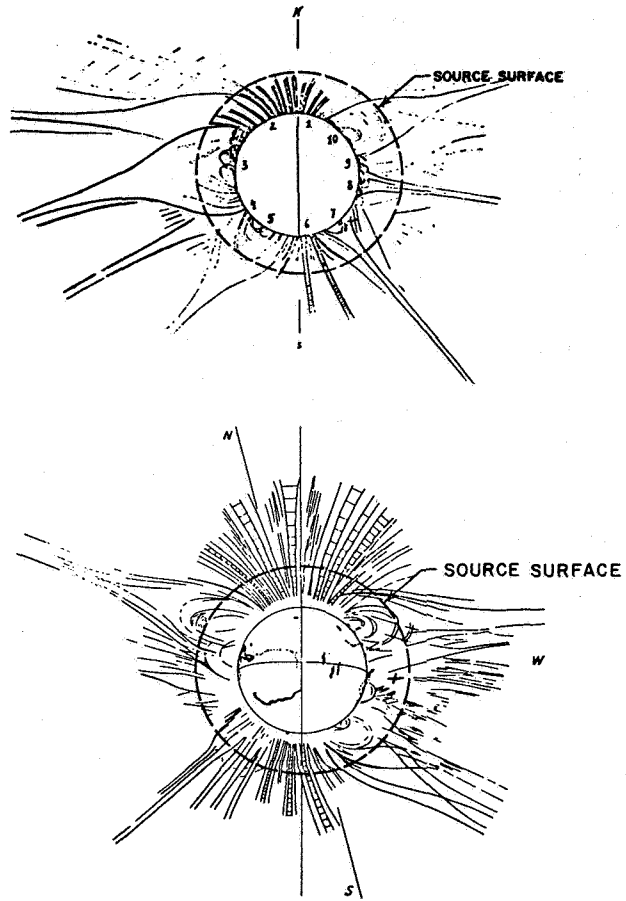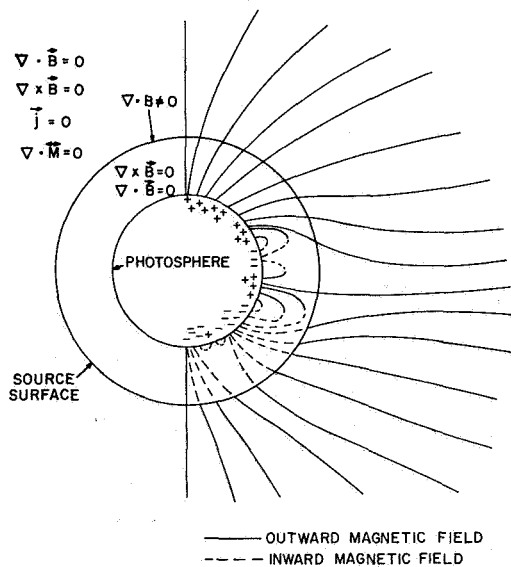

Figure 2. *Drawing of the February 15, 1961 solar eclipse (top) and the February 25, 1952 solar eclipse (bottom) superposed with a "source surface" at 1.6 solar radii. Note that most closed arches fall below this surface. Beyond this distance most structures are "open" but not strictly radially oriented.*

(providing transverse pressure stresses) falls off much less rapidly than that of the transverse field [Schatten et al. 1969]. The energy density of the transverse field approximately equals that of the plasma at about 0.6 solar radii (above the photosphere). Thus the plasma extends the magnetic field outward near this point. In the case of the radial field, quality with the plasma energy density is only reached at the Alfven point near 25 solar radii. Thus transverse magnetic pressure is expected to be an important effect long after the coronal plasma has become supersonic. The magnetic field behaves like open rigid wires along which the plasma is constrained to flow. The magnetic field thus may still guide the plasma motion from 0.6 to 25 solar radii. This paper suggests a method to mathematically calculate the magnetic structure in this region.
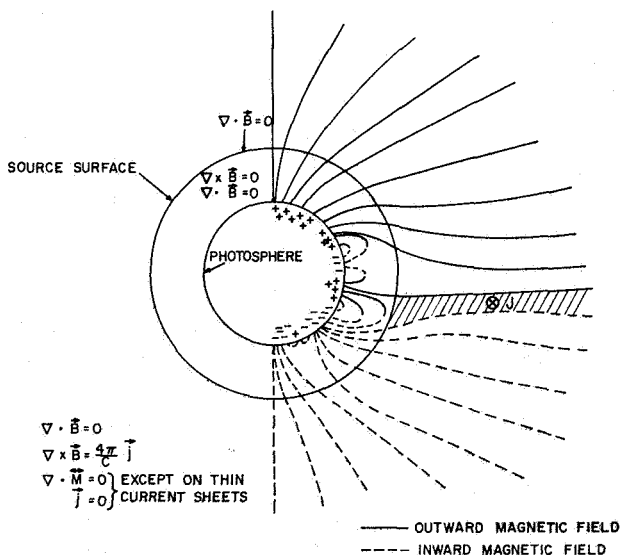
45

CURRENT SHEET MODEL

Out to the Alfvén point, the value of β (ratio of plasma to field energy density) for the coronal plasma is significantly less than one. Thus currents flowing in the coronal plasma cannot apply a significant pressure on the magnetic field except where the field is weak (near regions of opposite polarity fields). Currents are necessary to open the magnetic field into sector-like structures. If any significant transverse currents were located in regions of moderate field strength, a strong $j \times B$ force would occur which the plasma could not resist. Thus, the currents tend to be present in high β regions, where the field reverses, and the $j \times B$ forces are small. For these reasons, the transverse currents flowing in the coronal plasma in this model are constrained to flow only where the field is weak (near zero), hence on sheets near oppositely directed field regions.

The magnetic model can be used for computing the location and strength of these current sheets as follows. The magnetic field is first calculated directly from potential theory by means of Legendre polynomial techniques to a particular surface — for example, a sphere of radius 1.6 solar radii. Although not utilized in exactly the same way, this sphere will again be referred to as the "source surface." The magnetic field then is reoriented

such that it points outward everywhere; however, it is still along the same direction and possesses the same field magnitude. Thus if $B_r \geqslant 0$ on this "source surface" the field is unchanged, but if $B_r < 0$ then B_r, B_θ, and B_Φ are replaced by $-B_r$, $-B_\theta$, and $-B_\phi$. The field is then calculated beyond the "source surface" from potential theory, again using a Legendre polynomial expansion of the field (see appendix). Now the monopole term is non-zero and rather large; thus it appears as if the sun has a high magnetic monopole moment and all the Legendre polynomial coefficients bear little or no relationship to their previous values (fig. 3). The physical effect is that beyond the "source surface" the magnetic fields cannot now form closed arches as they are all directed outward. This temporarily violates $\nabla \cdot B = 0$ on the source surface but this error will be corrected in a later step. This change of field direction does not affect the magnetic stresses: They will remain the same across the "source surface" and the field will still form a minimum energy configuration (with the condition that the field lines remain open). The last step (fig. 4) is to return the

———— OUTWARD MAGNETIC FIELD
— — — INWARD MAGNETIC FIELD

Figure 3. *First step in the current sheet magnetic model. A potential solution is derived for the field between the "source surface" and the photosphere. The field computed on the source surface is then reoriented so that it points outward everywhere. The field is then computed beyond the "source surface" from potential theory. The sense of the magnetic field is opposite half the time to what it should be. This "error" is corrected in the next step.*

———— OUTWARD MAGNETIC FIELD
— — — INWARD MAGNETIC FIELD

Figure 4. *Second step in the current sheet magnetic model. The field that was disoriented is reoriented by reversing the sense of the magnetic field components. This requires a current sheet to be employed in the corona to separate regions of oppositely directed field to obey Maxwell's equations. Allow the magnetic field to "open" by thin current sheets is consistent with the physical model of this region of the corona possessing a low β. If significant transverse currents flowed elsewhere a strong $j \times B$ force would develop which the plasma could not maintain. This model may be used to calculate the magnetic oriented structures in the corona with less simplified solar wind currents.*

46

magnetic field to its former sense of direction with the calculated strength and orientation. This violates $\nabla \times \mathbf{B} = 4\pi\mathbf{j}/C = 0$ unless appropriate current sheets are introduced as shown. Physically, current sheets are introduced between areas of oppositely directed fields and thus prevent the field from forming arches beyond the "source surface." Note that the polar fields and streamer fields possess similar shapes to those in the corona (fig. 2) and not the radial orientation seen in figure 1.

The invariance of the Maxwell stress tensor under this field reversal scheme is important to ensure against unequal stresses across the "source surface." The Maxwell stress tensor is defined such that $\mathbf{j} \times \mathbf{B} = \nabla \cdot \mathbf{M}$. The stress tensor is shown in figure 5. As can be seen, changing the sign of the three components leaves $\mathbf{M}$ unchanged; thus, the magnetic stresses in the corona are balanced.

$$\vec{j} \times \vec{B} = \nabla \cdot \overleftrightarrow{M}$$

$$\overleftrightarrow{M} = \frac{1}{\mu_0} \begin{bmatrix} \frac{1}{2}(B_X^2 - B_Y^2 - B_Z^2) & B_X B_Y & B_X B_Z \\ B_X B_Y & \frac{1}{2}(B_Y^2 - B_X^2 - B_Z^2) & B_Y B_Z \\ B_X B_Z & B_Y B_Z & \frac{1}{2}(B_Z^2 - B_X^2 - B_Y^2) \end{bmatrix}$$

Figure 5. *The Maxwell stress tensor. Note that it is identical if all three components are reversed. This allows the stresses to be balanced after the field reversal processes.*

COMPARISONS OF THE CURRENT SHEET MODEL WITH OTHER MODELS AND THE SOLAR CORONA

The current sheet model is first compared with the "source surface" and the "zero potential surface" models as well as an exact MHD solution for an axisymmetric isothermal corona. This latter solution has been computed after the formalism of *Pneuman and Kopp* [1970] for the corona with a temperature of 1.56×10^6 °K and a dipole field. Figure 6 shows this comparison with an assumed dipolar solar field. The field lines labeled with crosses represent the present study with the "source surface" located at 1.6 solar radii. Solid lines indicate field directed away from the sun, and dashed lines indicate field toward the sun. The heavy solid lines indicate the MHD isothermal coronal solution of Pneuman and Kopp. The dashed and dotted lines indicate the field lines calculated by the Altschuler and Newkirk model with a zero potential surface located at 2.5 solar radii. The "source surface" solution of *Schatten et al.* [1969] is similar to this solution except the field lines would be oriented radially somewhat closer to the sun. As can be seen, the field lines computed from the isothermal MHD solution and the current sheet solution are nearly identical. The foot points
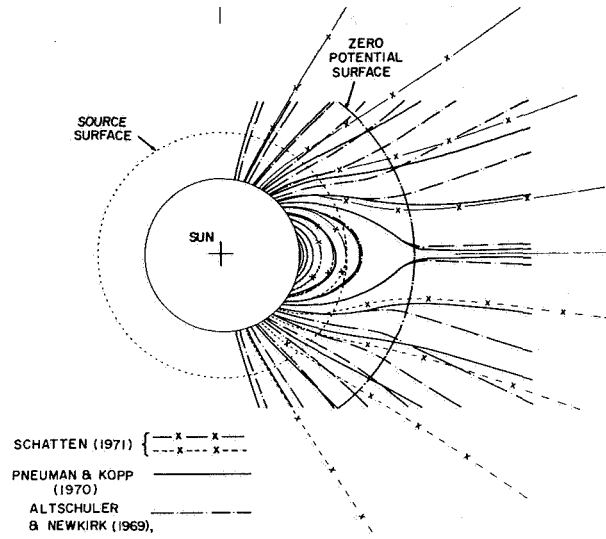

Figure 6. *A comparison of solutions for a dipole solar field with the zero potential surface model [Altschuler and Newkirk, 1969] the present model and the exact isothermal MHD coronal solution [Pneuman and Kopp, 1970]. Note that the present solution is quite similar to the isothermal coronal solution supporting the suggestion that the coronal currents are confined to thin sheets.*

of the field lines indicate the quality of their agreement. The magnetic potential solution begins to diverge from the other solutions near the zero potential surface. The rather close agreement between the current sheet solution and the MHD solution suggests that much of the current flowing in an isothermal corona does so near current sheets as suggested earlier. *Altschuler and Newkirk* [1969] chose the location of the zero potential sphere to be 2.5 solar radii based on a comparison of field geometry with coronal forms, whereas *Schatten et al.* [1969] chose the 1.6 solar radii value for the "source surface" based upon the observed highest closed arches and agreement with comparisons of their model with the interplanetary magnetic field. In the present model, if the "source surface" is set at 1.6 solar radii, the shapes of features are similar (out to 2+ solar radii) to the Altschuler and Newkirk result, and the coronal magnetic field extends out from 1.6 solar radii, similar to the result of *Schatten et al.* [1969]. Thus the disagreement between these two values where the coronal magnetic fields extends outward may be ended by utilizing this new model. The agreement with the axisymmetric MHD solution suggests that the current sheet model may now be used with more confidence in calculating fields in three dimensional nonsymmetric situations as well.

First, however, let us examine whether the current

sheet model can calculate nonradial streamers and compare them with observed nonradial streamers. Figure 7 is a drawing from Bohlin of the May 30, 1965, solar eclipse from photographs by Smith (top). This eclipse shows several nonradial streamers in addition to the nonradial polar plumes. The field pattern beneath shows calculations from the current sheet model using an axisymmetric magnetic condition. As can be seen, rather nonradial field lines may be computed in the model quite similar in appearance to the structures observed. The

N

Extends to $\geq$ 10 $R_{\odot}$

E

W

30 May, 1965

S
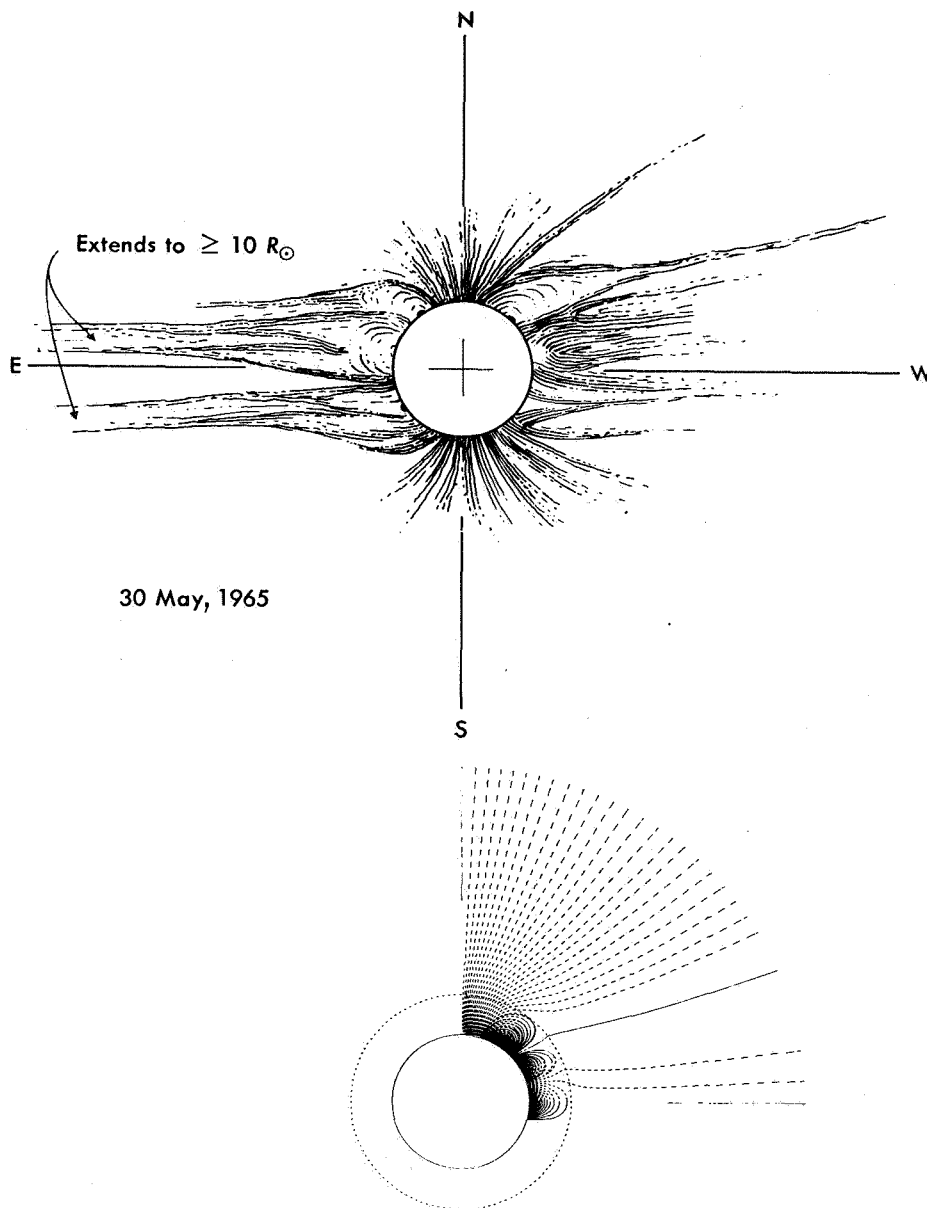
Figure 7. *A comparison of the structure of the solar corona during the May 30, 1965 solar eclipse (top) with computations from an assumed axisymmetric photospheric field pattern (bottom). The shape of the polar plumes is calculated quite well in this model as well as a nonradial helmet streamer.*

48

polar field lines appear similar to the polar plumes. The computed field configuration in the equatorial regions are also oriented toward the equator as in the eclipse drawing.

A computation of the magnetic field projected into the plane of the sky from this model for the November 12, 1966, solar eclipse is shown in figure 8 superimposed with a drawing of the coronal forms by *Newkirk et al.* [1970]. The solid lines indicate away-from-the-sun magnetic field, and dashed lines indicate toward-the-sun field. Many of the features line up surprisingly well with the field lines calculated as can be seen. Large-scale magnetic loops are calculated near streamers β' and ζ and closed arches are observed underlying these streamers. Many of the "open" magnetic field lines near regions β, ζ, and γ are closely alined with coronal features in the same areas. The general agreement of the magnetic field calculations with the observed features for this solar eclipse is rather good.

CONCLUSIONS

A new current sheet magnetic model for the solar corona
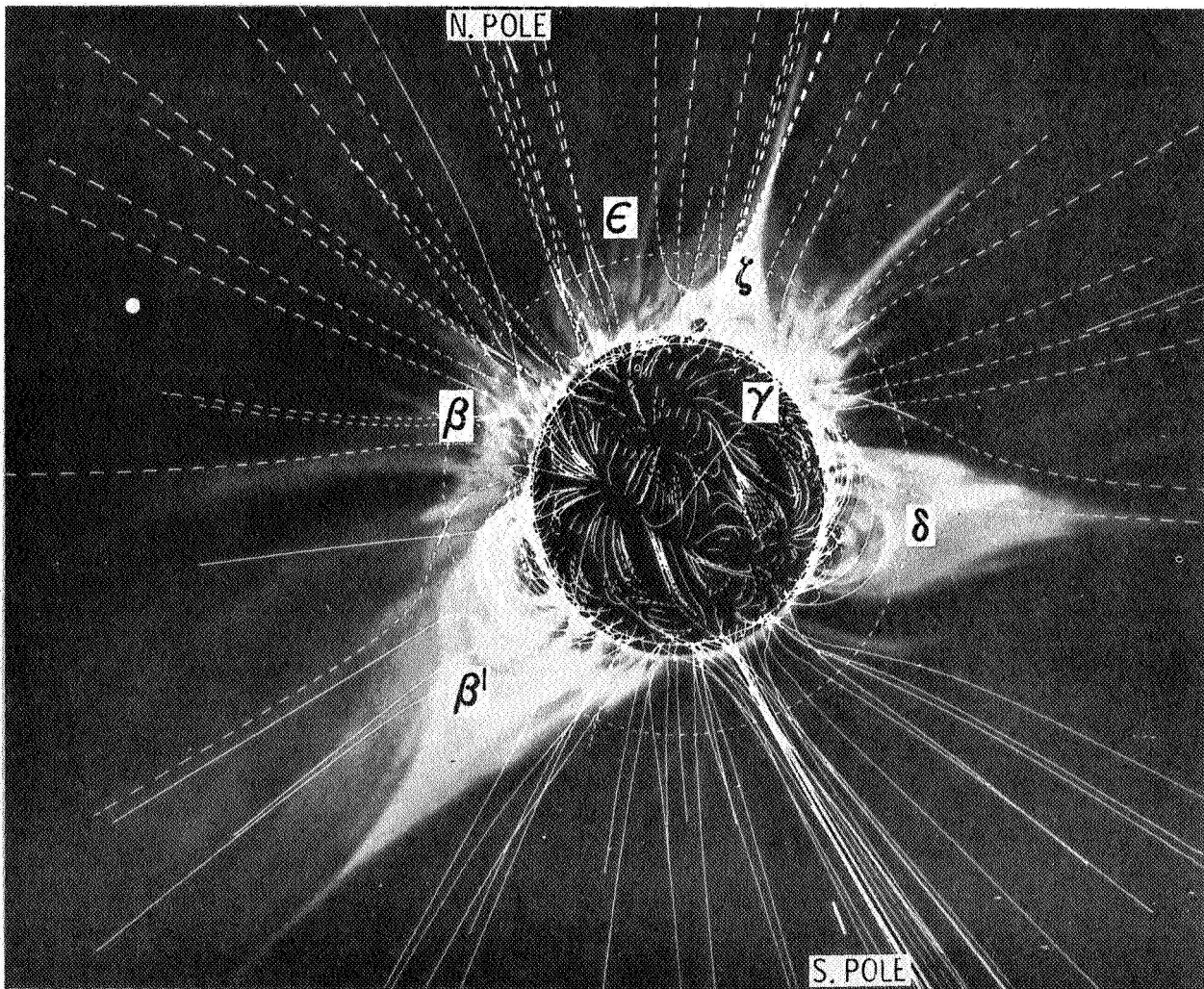
Figure 8.   *A comparison of the computed coronal magnetic field with a drawing of the solar eclipse features from Newkirk and Altschuler* [1970] *for the November 12, 1966 solar eclipse. The solid lines represent magnetic field directed away from the sun and the dashed lines field toward the sun. The field lines originate on the photosphere in the center of each of the 648 grid points. Many of the observed features line up with the computed field lines. The computed field lines terminate at five solar radii and are projected into the plane of the sky.*

has been developed. It is capable of calculating the quiet large-scale magnetic field structure in the corona. As suggested by physical arguments, thin current sheets are utilized to separate regions of oppositely directed fields. This approximation appears to be a rather good one in that the dipole solution is nearly identical with the isothermal MHD coronal solution of *Pneuman and Kopp* [1970].

A comparison of field computations with the observed structure for the May 30, 1965, solar eclipse reveals that the model appears to be capable of calculating the orientation of the polar plumes fairly well, as well as nonradial streamer configurations. A comparison between the computed magnetic field and the observed solar corona for the November 12, 1966, solar eclipse is shown. Many of the observed features are also seen in the computed magnetic field.

APPENDIX   This appendix discusses the solution of the field beyond the "source surface" method of fitting the vector Legendre polynomial coefficients to the three dimensional vector field on the "source surface." The vector field up to and including the "source surface" is computed in accord with the techniques of *Altschuler and Newkirk* [1969] without using any currents in the solar corona. The present model may be improved in the future by an iterative process using the currents computed in the present model to calculate the solution below the "source surface" as well and then recomputing the field beyond the "source surface." This may represent a minimum improvement, however.

The solution for the Laplacian equation in spherical coordinates for $r \geq R$ is

$$\psi(r,\theta,\phi) = R \sum_{n=o}^{\infty} \sum_{m=o}^{n} \left\{ \left(\frac{R}{r}\right)^{n+1} \left[g_n^m \cos(m\phi) + h_n^m \sin(m\phi) \right] P_n^m(\theta) \right\} \tag{1}$$

The components of the magnetic field are:

$$B_r = -\frac{\partial \psi}{\partial r} = f_1(g_n^m, h_n^m) \tag{2}$$

$$B_\theta = -\frac{\partial \psi}{r\, \partial \theta} = f_2(g_n^m, h_n^m) \tag{3}$$

$$B_\phi = -\frac{1}{r \sin \theta} \frac{\partial \psi}{\partial \phi} = f_3(g_n^m, h_n^m) \tag{4}$$

The associated Legendre polynomials utilizing the Schmidt normalization have been used [*Chapman and Bartels*, 1940]. Thus to determine the magnetic field beyond the "source surface" it is necessary to compute g_n^m and h_n^m from the vector field on the "source surface" as a boundary condition.

The components of the magnetic field on the "source surface" are first oriented away-from-the sun so that if $B_r < 0$ on the "source surface," the signs of B_r, B_θ, and B_ϕ are reversed.

In this analysis we have utilized a photospheric grid of 27 longitudes and 24 latitudes in equal steps of sinc (latitude). We have also chosen $N = 9$ as the maximum principal Legendre index to consider for practical considerations. A least-mean-square fit to an overdetermined linear system of 1944 (27X24X3) equations involving 100 unknowns is then utilized to best fit the vector field on the "source surface," we let

$$F = \sum_{i=1}^{24} \sum_{j=1}^{27} \sum_{k=1}^{3} \left[B(i, j, k) - f_k(g_n^m, h_n^m) \right]^2 \tag{5}$$

where $B(i,j,k)$ equal the vector field components, and $k = 1, 2,$ or 3 refers to the radial, latitudinal, or azimuthal field component at θ_i and ϕ_j.

It is necessary now to obtain the g_n^m and h_n^m that minimize F; the sums of squares of the differences between the known components of the field on the "source surface" $B_r(i,j)$, $B_\theta(i,j)$ and $B_\phi(i,j)$; and the component values computed from g_n^m and h_n^m at θ_i and ϕ_j.

Let us choose

$$\left.\begin{array}{l}
\alpha_{nm1} = (n + 1)\cos m\phi \; P_n^m(\theta) \\[12pt]
\beta_{nm1} = (n + 1)\sin m\phi \; P_n^m(\theta) \\[12pt]
\alpha_{nm2} = -\cos m\phi \; \dfrac{d}{d\theta} \; P_n^m(\theta) \\[12pt]
\beta_{nm2} = -\sin m\phi \; \dfrac{d}{d\theta} \; P_n^m(\theta) \\[12pt]
\alpha_{nm3} = \dfrac{m}{\sin \theta} \; \sin m\phi \; P_n^m(\theta) \\[12pt]
\beta_{nm3} = \dfrac{m}{\sin \theta} \; \cos m\phi \; P_n^m(\theta)
\end{array}\right\} \tag{6}$$

Thus equation (5) becomes

$$F = \sum_i \sum_j \sum_k \left[B(i, j, k) - \sum_n \sum_m \left(g_n^m \; \alpha nmk + h_n^m \; \beta nmk \right) \right]^2 \tag{7}$$

The equations to minimize F are:

$$\frac{\partial F}{\partial g_n^m} = 0 \quad \frac{\partial F}{\partial h_n^m} = 0 \tag{8}$$

For each (n, m) may be rewritten:

$$\sum_i \sum_j \sum_k \left\{ B(i, j, k)\alpha_{nmk}(ij) - \alpha_{nmk}(ij) \sum_{t=0}^{N} \sum_{s=0}^{t} \left[g_t^s \alpha_{tsk}(ij) + h_t^s \beta_{tsk}(ij) \right] \right\} = 0 \tag{9}$$

$$\sum_i \sum_j \sum_k \left\{ B(i, j, k)\beta_{nmk}(ij) - \beta_{nmk}(ij) \sum_{t=0}^{N} \sum_{s=0}^{t} \left[g_t^s \alpha_{tsk}(ij) + h_t^s \beta_{tsk}(ij) \right] \right\} = 0 \tag{10}$$

where t and s are dummy indices used for n and m. The unknowns are g_n^m and h_n^m, and $B(i,j,k)$ is the known vector field; α and β are known from equation (6).

The column vectors

$$\alpha_{NM} = \begin{bmatrix} \alpha_{\theta_1 \phi_1 1} \\ \alpha_{\theta_1 \phi_2 1} \\ \cdot \\ \cdot \\ \cdot \\ \alpha_{\theta \phi 1} \\ \alpha_{\theta_1 \phi_1 2} \\ \cdot \\ \cdot \\ \cdot \\ \alpha_{\theta \phi 3} \end{bmatrix} \qquad \beta_{NM} = \begin{bmatrix} \beta_{\theta_1 \phi_1 1} \\ \beta_{\theta_1 \phi_2 1} \\ \cdot \\ \cdot \\ \cdot \\ \beta_{\theta \phi 1} \\ \beta_{\theta_1 \phi_1 2} \\ \cdot \\ \cdot \\ \cdot \\ \beta_{\theta \phi 3} \end{bmatrix} \left. \rule{0pt}{9em} \right\} \tag{11}$$

are of length $24 \times 27 \times 3$ for each NM and

$$\mathbf{B} = \begin{bmatrix} B(\theta_1, \phi_1, 1) \\ B(\theta_1, \phi_2, 1) \\ \cdot \\ \cdot \\ \cdot \\ B(\theta, \phi, 1) \\ B(\theta_1, \phi_1, 2) \\ \cdot \\ \cdot \\ \cdot \\ B(\theta, \phi, 3) \end{bmatrix} \qquad \mathbf{GH} = \begin{bmatrix} g_0^0 \\ g_1^0 \\ g_1^1 \\ \cdot \\ \cdot \\ \cdot \\ g_N^N \\ h_1^1 \\ h_2^1 \\ \cdot \\ \cdot \\ \cdot \\ h_N^N \end{bmatrix}$$

Now defining the matrix $\alpha\beta$ such that the rows of $\alpha\beta$ are as follows:

$$\alpha\beta(1) = \alpha_{0\,0}$$

$$\alpha\beta(2) = \alpha_{1\,0}$$

$$\alpha\beta(3) = \alpha_{1\,1}$$

$$\ldots$$

$$\alpha\beta(55) = \alpha_{9\,9}$$

$$\alpha\beta(56) = \beta_{1\,1}$$

$$\ldots$$

$$\alpha\beta(100) = \beta_{9\,9}$$

with all $m = 0$ elements missing from h_n^m and from β; **GH** is a 100×1 matrix and $\alpha\beta$ is a 100×1944 matrix. Equations (9) and (10) may be rewritten as

$$A\beta \cdot \mathbf{B} = AB \cdot \mathbf{GH} \tag{12}$$

choosing $AB(i,j) = \alpha\beta(i) \cdot \alpha\beta(j)$ so that $\alpha\beta$ is a 100×1944 matrix, **B** is a 1944×1 matrix, AB_{ij} is a 100×100 matrix and **GH** is a 100×1 matrix.

By an inversion of the symmetric matrix AB, **GH** may be solved as follows:

$$\mathbf{GH} = AB^{-1} \cdot \alpha\beta \cdot \mathbf{B}$$

This requires inverting a square matrix each of whose sides equals $(N+1)^2$ which for $N = 9$ is 100, yielding estimates for g_n^m and h_n^m that arise from a least mean square fit to the three vector components of the magnetic field on the source surface. Equations (2), (3), and (4) allow a computation of the magnetic field everywhere above the "source surface." It is necessary, however, to reverse the sense of the three components of the magnetic field depending on whether the footpoint of the field line has had its sense reversed (if $B_r < 0$). Those field lines are shown as dashed lines in the figures.

REFERENCES
Altschuler, M. D.; and Newkirk, G., Jr.: Magnetic Fields and the Structure of the Solar Corona. *Solar Physics,* Vol. 9, 1969, p. 131.

Bugoslavaskaya, E. Ya.; Trud. Gos. Astronom. Inst. in Shternberga, Vol. 19, 1950, p. 3.

Chapman, S.; and Bartels, J.: *Geomagnetism.* Oxford University Press, London, 1940.

Cowling, T. G.; The Solar Wind. *The Observatory,* Vol. 89, 1969, p. 217.

Gold, T., The Magnetic Field in the Corona. *IAU Symposium No. 6,* 1956, p. 275.

Newkirk, G.A., Jr.: *Ann. Rev. Astron. and Astrophys.* Vol. 5, 1967, p. 213.

Newkirk, G. A., Jr.; Altschuler, M. D,; and Harvey, J. W.: Influence of Magnetic Fields on the Structure of the Solar Corona. *Structure and Development of Solar Active Regions* (ed. by K. O. Kiepenheuer) *IAU Symposium No. 35,* D. Reidel Publ. Co., Dordrecht, 1968, p. 379.

Newkirk, G. A., Jr.; Schmahl, E.; and Deupree, R.: Magnetic Fields and the Structure of the Solar Corona II: Observations of the 12 November 1966 Solar Eclipse. *Solar Physics,* Vol. 15, 1970, p. 15.

Pneuman, G. W.; and Kopp, R. A.: Coronal Streamers III: Energy Transport in Streamer and Interstreamer Regions. *Solar Physics,* Vol. 13, 1970, p. 176.

Rust, D. M.: Measurements of the Magnetic Fields in Quiescent Solar Prominences. Ph.D. thesis, University of Colorado, 1966.

Schatten, K. H. : Large-Scale Configuration of the Coronal and Interplanetary Magnetic Field. *Thesis,* University of California, Berkeley, 1968a.

Schatten, K. H.: Prediction of the Coronal Structure for the Solar Eclipse of September 22, 1968. *Nature,* Vol. 220, 1968b, p. 1211.

Schatten, K. H.: Coronal Structure at the Solar Eclipse of September 22, 1968. *Nature,* Vol. 223, 1969, p. 652.

Schatten, K. H.: Prediction of the Coronal Structure for the Solar Eclipse of March 7, 1970. *Nature,* Vol. 226, 1970, p. 251.

Schatten, K. H.; Wilcox, J. M.; and Ness, N. F.: A Model of Coronal and Interplanetary Magnetic Fields. *Solar Physics,* Vol. 9, 1969, pp. 442-455.

Schmidt, H. U.: On the Observable Effects of Magnetic Energy Storage and Release Connected with Solar Flares. *AAS-NASA Symposium Phys. Solar Flares,* ed. W. N. Hess, NASA-SP-50, 1964, p. 107.

Smith, S. M., and Schatten, K. H.. *Nature,* Vol. 226, 1970, p. 1130.

Stelzried, C. T.; Levy, G. S.; Sato, T.; Rusch, W. V. T.; Ohlson, J. E.; Schatten, K. H.; and Wilcox, J. M.: *Solar Physics,* Vol. 14, 1970, p. 440.

Takakura, T.: *Space Science Reviews.* Vol. 5, 1966, p. 80.

Waldmeier, M.: *Nature.* Vol. 226, 1970, p. 1131.

DISCUSSION

R. A. Kopp I just wanted to know how you got the field lines to go through the source surface radially. You said you did that calculation first with the ordinary source surface. Don't the field lines have to go perpendicular as they pass through the source surface?

K. H. Schatten No, they weren't taken to be radial in this case. It was strictly a potential theory using the Legendre polynomial coefficients, and we did not constrain them to be radial — they just occur in whatever direction they happen to be there. Then we did a least-mean-square solution so that the three vectors, B_r B_Θ B_ϕ, are at the source surface, so that there was no necessary restriction into the radial direction there.

R. B. Leighton It's a kind of heuristic way of recognizing you're going from a case where there is essentially a potential magnetic field problem to a fluid problem but in which the magnetic field still plays a role in terms of its stress, in guiding the flow. This is why you get away with reversing the field there and keeping on going and damn the torpedoes — right?

K. H. Schatten Right.

F. C. Michel I don't know if it's directed to Ken Schatten or to Gordon Newkirk. But the eclipse of 1970 looked quantatively as if it had been drawn by a student who hadn't learned his lessons very well, and if he had drawn it in the form it appeared he would be critized for having a rather poor representation of how the lines should go. There are great regions where the striations are essentially parallel; and not only that but they didn't appear at all radially from the sun, and there were about five such regions. I just wondered, what's your attitude towards this? Do you think this is a significant deviation from the theory or do you think that's easy to account for?

K. H. Schatten Yes, I think it is a significant deviation. As Gordon Newkirk mentioned, there was a lot of solar activity at the time. These models essentially assume quasistationary conditions with no sort of solar activity to mess things up. When you have activity you get a lot of plasma ejected into the corona, and currents can form which will twist the field to almost any configuration, and you can't just compute it from the photospheric field. You can imagine a very strong flare occurring in a particular location where you have, say, a stream or something like that, and it blows all the field lines out into radially away from that point, or into some other configuration. That probably is why the solar eclipse calculations for 1970 were not as good as some of the others.